MICROBIOLOGY

Circadian clock is critical for fungal pathogenesis by regulating zinc starvation response and secondary metabolism

Qiaojia Lu[1,2]†, Muqun Yu[1]†, Xianyun Sun[1,2]†, Xin Zhou[1], Rui Zhang[1], Yahao Zhang[1,2], Xiao-Lan Liu[1], Zhanbiao Li[3], Lei Cai[1,2], Hongwei Liu[1], Shaojie Li[1,2], Yunkun Dang[3], Xiaodong Xu[4], Qun He[5], Yi Liu[6], Xiao Liu[1,2]*

Circadian clocks are known to modulate host immune responses to pathogen infections, yet their role in influencing pathogen pathogenesis remains unclear. Here, we investigated the role of circadian clocks in regulating the pathogenesis of the fungal pathogen *Fusarium oxysporum*, which has multiple genes homologous to the *Neurospora crassa frq* due to gene duplication events, with *Fofrq1* being the primary circadian clock gene. The pathogenesis of *F. oxysporum* in plants is controlled by its circadian clock, with infections causing severe disease symptoms at dawn. Notably, disruption of clock genes dramatically reduces fungal pathogenicity. Circadian clocks regulate the rhythmic expression of several transcription factors, including FoZafA, which enables the pathogen to adapt to zinc starvation within the plant, and FoCzf1, which governs the production of the toxin fusaric acid. Together, our findings highlight the critical roles of circadian clocks in *F. oxysporum* pathogenicity by regulating zinc starvation response and secondary metabolite production.

INTRODUCTION

Circadian clocks are time-regulating systems that operate in organisms ranging from bacteria to humans. They play a crucial role in coordinating biological processes by controlling the rhythmic expression of genes, enabling adaptation to daily changes of environments (*1*–*3*). The eukaryotic circadian clocks depend on core oscillators driven by transcription-translation–coupled negative feedback loops (*2*, *4*, *5*). The nonpathogenic fungus *Neurospora crassa* is a major eukaryotic model system for chronobiology studies (*5*). In the core oscillator of *N. crassa* circadian system, the transcription factor/photoreceptor white collar-1 (WC-1) associates with white collar-2 (WC-2) to form the white collar complex (WCC), which periodically binds to the *C-box* site in the promoter of the *frequency* (*frq*) gene, rhythmically activating the expression of *frq* (*6*–*8*). FRQ associates with its partner, FRQ-interacting RNA helicase (FRH), forming the FRQ-FRH complex and acts as the negative element of the negative feedback loop that inhibits the transcription of *frq* by inhibiting the activity of WCC (*9*–*11*). FRQ undergoes progressive phosphorylation by kinases and subsequent degradation, and the ability of FRQ to be phosphorylated determines the period of circadian cycle (*12*–*15*). Therefore, FRQ plays a key role in the circadian clock system.

Although some fungal species have a single gene encoding for protein homologous to *N. crassa* FRQ, some fungal genomes do not have *frq* gene. The role of the circadian clock and FRQ homologs has been extensively investigated in *Neurospora*, but research on their functions in pathogenic fungi remains limited. In *Aspergillus flavus*, a circadian oscillator was found to rhythmically regulate the development of sclerotia (*16*). In *Botrytis cinerea*, it was shown that the fungal clock influences its interaction with the plant *Arabidopsis* and regulates the fungal-fungal interaction with *Trichoderma atroviride* (*17*, *18*). However, in *Verticillium dahliae*, the existence of a functional circadian clock is unclear although it contains all components of circadian core oscillators (*19*, *20*). Thus, while circadian clock function has been described in several fungi, only a small number of pathogenic fungi have been validated to have functional circadian clocks, and the mechanisms underlying circadian clock control of fungal pathogenicity are unknown (*21*, *22*).

Fusarium oxysporum is a pathogen that causes a wide range of diseases in plants including melons, cotton, and Solanaceae, among others (*23*, *24*). *F. oxysporum* ranks fifth among the top 10 plant pathogenic fungi due to its broad pathogenicity (*25*). Full immune system mobilization is required for plants to cope with *F. oxysporum* invasion. The preexisting plant defense system includes physical and chemical barriers against pathogen penetration (*26*, *27*). Once *F. oxysporum* overcomes these defenses, its general pathogenicity factors induce pathogen-associated molecular pattern–triggered immunity in hosts, an immune response that relies on transmembrane pattern recognition receptors (*24*, *28*). Moreover, the plant activates effector-triggered immunity by recognizing secreted effectors to protect itself from phytotoxins, which are products of the secondary metabolism of *F. oxysporum* (*27*, *28*). Comparative genomic analysis has revealed that the *F. oxysporum* genome is divided into core chromosomes (for primary metabolism and reproduction) and accessory chromosomes (for pathogen virulence, host specialization, and potentially other functions) (*29*). Wide pesticide use against *F. oxysporum* has selected for the emergence of drug-resistant strains, indicating an urgent need for new strategies to combat this pathogen (*30*).

Although the functions of the circadian clock in the host immune system and the regulation of the outcome of pathogen infection have been well documented (*31*–*34*), including those showing

[1]State Key Laboratory of Mycology, Institute of Microbiology, Chinese Academy of Sciences, Beijing, 100101, China. [2]College of Life Sciences, University of Chinese Academy of Sciences, Beijing, 100049, China. [3]School of Life Sciences, Yunnan University, Kunming, Yunnan, 650091, China. [4]State Key Laboratory of Crop Stress Adaptation and Improvement, School of Life Sciences, Henan University, Kaifeng, 475004, China. [5]MOA Key Laboratory of Soil Microbiology, College of Biological Sciences, China Agricultural University, Beijing, 100193, China. [6]Department of Physiology, University of Texas Southwestern Medical Center, Dallas, TX 75390-9040, USA.
*Corresponding author. Email: liux@im.ac.cn
†These authors contributed equally to this work.

that the circadian clock regulates virulence in the plant pathogenic fungi and the insect-controlling fungi (*17*, *22*, *35*, *36*), the role played by circadian clocks of pathogens in their pathogenicity remains unclear. Here, we used plant pathogen *F. oxysporum* to elucidate the function of the fungal circadian clock in virulence and host-pathogen interaction. The genome of *F. oxysporum* is predicted to encode multiple FRQ homologs (*37*). Our study reveals the existence of a functional circadian clock in *F. oxysporum*. Our results demonstrate that the circadian clock in *F. oxysporum* plays a critical role in its pathogenicity by controlling fungal response to zinc starvation and secondary metabolite production.

RESULTS

F. oxysporum has a functional circadian clock

To identify potential circadian clock genes in *F. oxysporum* f. sp. *lycopersici*, we examined its genome for homologs of circadian clock components from *N. crassa*. Two homologs, FoWC1 (FOXG_03727) and FoWC2 (FOXG_01037), were identified as counterparts to *N. crassa* WC-1 and WC-2. For FRQ, we identified 10 FoFRQ proteins (FRQ homologs) (*37*). Among these, FoFRQ1 (FOXG_07759), which shares 81% sequence identity with *N. crassa* FRQ, contains all the essential domains required for FRQ function (Fig. 1A). In addition, we found paired FRQ homologs with remarkably high sequence similarity: FoFRQ3 (FOXG_15104) and FoFRQ4 (FOXG_14378), FoFRQ5 (FOXG_15157) and FoFRQ6 (FOXG_14323), as well as FoFRQ7 (FOXG_16752) and FoFRQ8 (FOXG_16689) are nearly identical to one another (Fig. 1A). The number of FRQ homologs varies among the different forma specialis of *F. oxysporum*. Evolutionary analysis suggests that these FRQ homologs emerged within the *F. oxysporum* species and may have been transferred between different forma specialis (fig. S1A). Collinearity analysis revealed that these FRQs are associated with intraspecific gene duplications (Fig. 1B). Transcriptional analysis showed that *Fofrq1* exhibited the highest expression levels among the genes encoding FRQ homologs—more than 100 times greater than the other *Fofrq* genes (Fig. 1C). This finding suggests that *Fofrq1* may serve as the dominant FRQ in *F. oxysporum*.

Under free-running conditions in constant darkness (DD), both *Fofrq1* mRNA and protein levels oscillated rhythmically (Fig. 1, D and E). In addition, rhythmic expression of *Fofrq10* mRNA was also observed (Fig. 1D), while the other *Fofrq* genes did not display rhythmic expression at mRNA levels (fig. S2, A to E). These findings suggest that multiple *Fofrq* genes contribute to the core oscillator, with *Fofrq1* being the primary regulator and others playing minor roles.

To monitor the circadian rhythm of *F. oxysporum* in vivo, we introduced a luciferase (LUC) reporter gene at the endogenous locus of *Fofrq1*, creating a translational fusion reporter that contains FoFRQ1-LUC through homologous recombination (*38*). This reporter was driven by the endogenous *Fofrq1* promoter. The wild-type (WT) strain displayed a robust circadian rhythm of luciferase activity, with a period of approximately 24 hours. However, this rhythm was disrupted and became arrhythmic in the Δ*Fowc1* strain (Fig. 1F and fig. S2F).

Next, we examined the response of *Fofrq1* expression to light and temperature. White light rapidly induced the expression of *Fofrq1* and *Fofrq10* mRNAs in *F. oxysporum* (fig. S3, A and B). Similarly, elevated temperatures led to an up-regulation of FoFRQ1 protein levels at both the peak and trough of its oscillations (fig. S3C), similar to the behavior of FRQ in *N. crassa* (*39*). These results indicate that the circadian oscillators in *F. oxysporum* can respond to light and temperature, despite its status as a well-known soilborne fungal pathogen.

Regulatory network in the circadian oscillator of *F. oxysporum*

To determine the composition of the *F. oxysporum* core oscillator, we constructed circadian clock knockout mutants, including Δ*Fowc1*, Δ*Fowc2*, Δ*Fowcc* (deletion of both *Fowc1* and *Fowc2*), and Δ*Fofrh*, and representative mutants Δ*Fofrq1* and Δ*Fofrq10*. FRH is an essential gene that plays an important role in the circadian clock and RNA exosome in *N. crassa* (*9*). However, the gene encoding for FoFRH has been successfully deleted in *F. oxysporum* and is not essential in the entomopathogenic fungi *Metarhizium robertsii* and *Beauveria bassiana*, suggesting that FRH fungal homologs are not required for RNA exosome function in some fungi (*40*, *41*). While the growth of mutant mycelium was unaffected compared to the WT, pigment production was altered (fig. S3D). In the absence of FoWCC, *Fofrq1* mRNA levels were reduced and lost their rhythmicity as expected (Fig. 2, A and B), as the rhythmic expression of *Fofrq1* depends on the binding of FoWCC to its promoter (Fig. 2C and fig. S3E).

Coimmunoprecipitation (co-IP) assays demonstrated that FoWC1 interacts with FoWC2, forming the positive regulatory complex FoWCC in *F. oxysporum* (Fig. 2D). Similar to observations in *N. crassa* (*7*, *42*), deletion of *Fofrq1* resulted in decreased *Fowc1* and *Fowc2* mRNA levels (Fig. 2E), indicating that FoFRQ positively regulates *Fowcc* expression. As expected, ectopic overexpression of *Fofrq1* under the control of a strong promoter disrupted the rhythms of endogenous *Fofrq1* and *Fofrq10* and suppressed their expression (Fig. 2, F and G). This suggests that FoFRQ1 inhibits the activity of FoWCC, thereby establishing the negative feedback loop within the circadian oscillator (*17*, *43*).

Furthermore, as seen in *N. crassa* (*9*), co-IP assays revealed that FoFRQ interacts with FoFRH to form a complex in *F. oxysporum* (Fig. 2H). The absence of FoFRH impaired the oscillation of *Fofrq1* mRNA (Fig. 2I), indicating that FoFRH is essential for the circadian clock function in *F. oxysporum*. Overall, these findings reveal that the circadian oscillator of *F. oxysporum* is composed of the positive components FoWC1 and FoWC2 and the negative components FoFRQs and FoFRH. Together, these elements form a circadian regulatory network that drives circadian rhythms.

Circadian clock of *F. oxysporum* controls its pathogenesis

The importance of the circadian clock for the growth and metabolism of nonpathogenic fungi is well established (*31*, *44*), but its role in pathogenic fungi, particularly its effect on virulence, remains mostly unresolved (*17*, *22*, *35*, *36*). To address this, we evaluated the ability of *F. oxysporum* clock mutants to infect tomato plants. The disease severity index (DSI) was calculated from 7 to 30 days postinoculation (*35*). Disruption of either the positive regulators (*Fowc1* and *Fowc2*) or the negative regulators (*Fofrq1* and *Fofrh*), which compromised the core oscillator, resulted in a

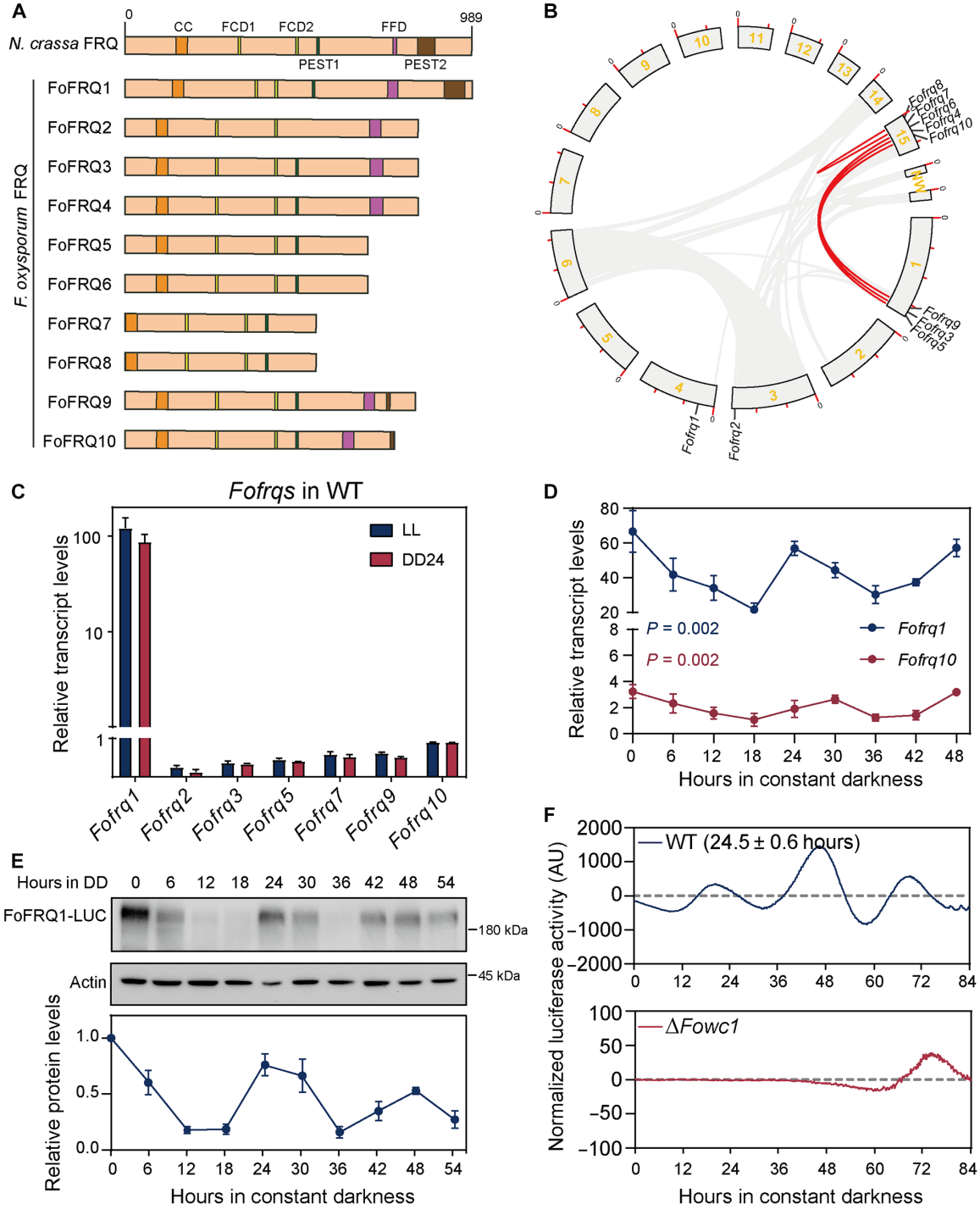

Fig. 1. FoFRQ1 is the main FRQ protein in the *F. oxysporum* circadian system. (**A**) Schematic representations of FoFRQ and NcFRQ proteins illustrate the lengths and structural domains. Previously defined functional domains include the coiled-coil domain (CC), FRQ–casein kinase I interacting domains (FCD1 and FCD2), FRQ-FRH interacting domain (FFD), and proline-, glutamate-, serine-, and threonine-rich sequence domains (PEST1 and PEST2). The FRQ homologous proteins include FoFRQ1 (FOXG_07759), FoFRQ2 (FOXG_14954), FoFRQ3 (FOXG_15104), FoFRQ4 (FOXG_14378), FoFRQ5 (FOXG_15157), FoFRQ6 (FOXG_14323), FoFRQ7 (FOXG_16752), FoFRQ8 (FOXG_16689), FoFRQ9 (FOXG_15043), FoFRQ10 (FOXG_14438), and FoFRQ-like (FOXG_22895). (**B**) The schematic of the chromosomal distribution and intrachromosomal relationships of *Fofrq* genes. Gray lines indicate all synteny blocks in the *F. oxysporum* genome, and red lines denote duplicated *Fofrq* gene pairs. (**C**) Reverse transcription quantitative polymerase chain reaction (RT-qPCR) quantification of *Fofrq* transcripts. Error bars indicate SDs ($n \geq 3$). (**D**) Relative transcript levels of *Fofrq* mRNAs. The eJTK_CYCLE algorithm was used to analyze the rhythmicity of gene expression, with $P < 0.05$ considered rhythmic. Error bars indicate SDs ($n \geq 3$). (**E**) Western blot analysis (top) and quantification (bottom) of FoFRQ1-LUC protein levels. Error bars indicate SDs ($n \geq 3$). (**F**) Quantification of luciferase signal from FoFRQ1-LUC in wild-type (WT; top) and Δ*Fowc1* (bottom) strains. AU, arbitrary units.

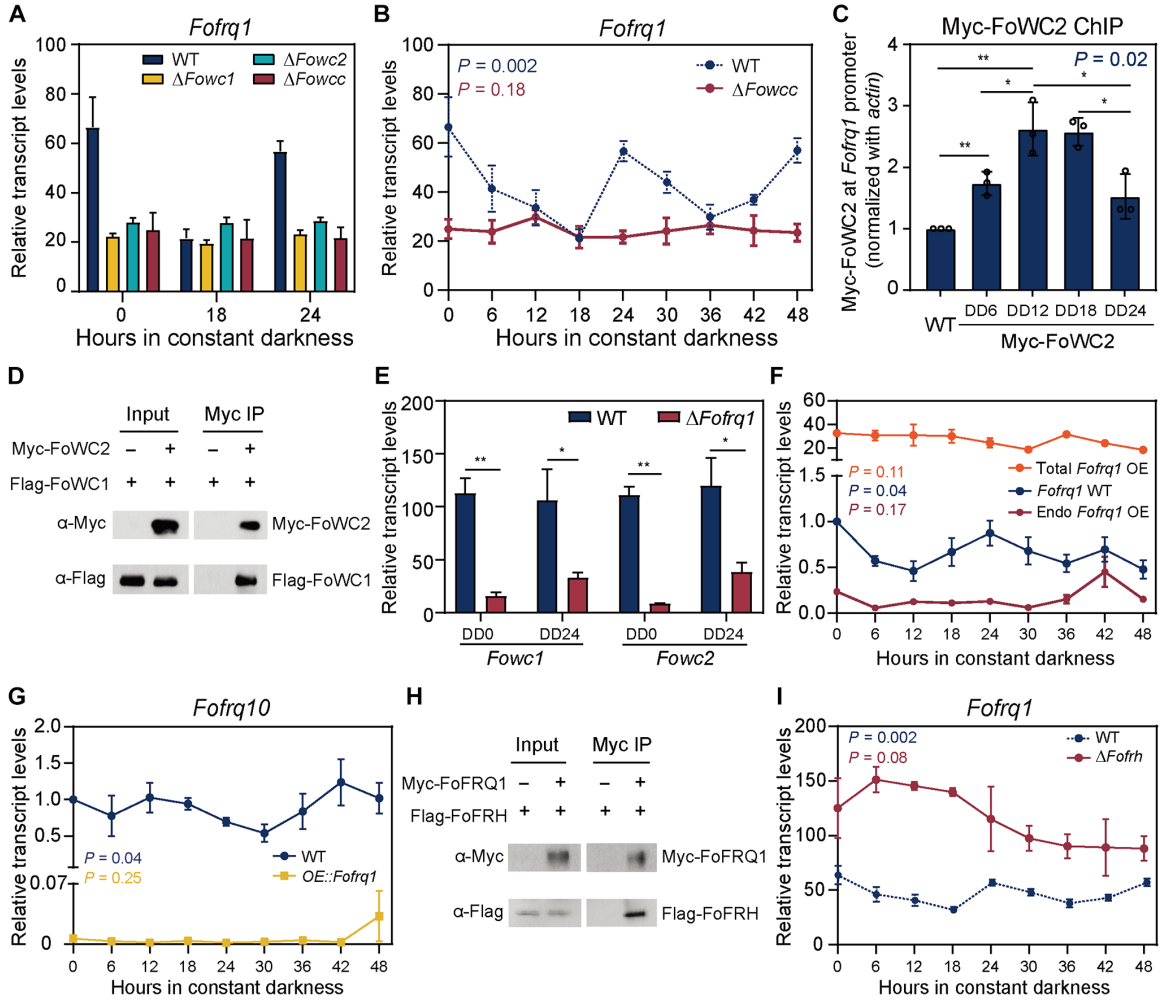

Fig. 2. Regulatory network of the circadian oscillator in *F. oxysporum*. (**A**) RT-qPCR analyses of *Fofrq1* mRNA levels in Δ*Fowc1*, Δ*Fowc2*, and Δ*Fowcc* strains. (**B**) RT-qPCR analyses of *Fofrq1* mRNA in the Δ*Fowcc* strain over time in DD. (**C**) Chromatin immunoprecipitation (ChIP)–qPCR assays of binding of FoWC2 to the promoter of *Fofrq1* at indicated times in DD. (**D**) Coimmunoprecipitation (co-IP) assays revealed the interaction between FoWC1 and FoWC2. (**E**) The mRNA levels of both *Fowc1* and *Fowc2* were diminished in the Δ*Fofrq1* mutant. (**F** and **G**) RT-qPCR analyses at indicated times in DD of (F) *Fofrq1* and (G) *Fofrq10* mRNAs in a strain that overexpresses *Fofrq1* (OE::*Fofrq1*). (**H**) Co-IP assays revealed the interaction between FoFRQ1 and FoFRH. (**I**) The mRNA level of *Fofrq1* was increased, and the rhythm of *Fofrq1* mRNA was impaired in the Δ*Fofrh* mutant. Error bars indicate SDs ($n \geq 3$). Student's *t* test was performed to determine statistical significance. $^*P < 0.05$ and $^{**}P < 0.01$.

nonpathogenic phenotype (Fig. 3A). In contrast, the Δ*Fofrq10* mutant still induced wilt symptoms (Fig. 3A), indicating that FoFRQ1, but not FoFRQ10, plays a pivotal role in fungal virulence.

Given the critical role of the circadian oscillator in *F. oxysporum*'s virulence, we hypothesized that its pathogenicity might exhibit diurnal variation. To test this, the tomato seedlings were grown under light-dark cycles (LD 12:12), but the fungal strains were cultured in either in-phase or opposite phase (antiphase) as the plants under LD (Fig. 3B). We inoculated tomato plants at lights-on time [host Zeitgeber time 0 (Host-ZT0)] and lights-off time [host Zeitgeber time 12 (Host-ZT12)] under LD (12:12) (Fig. 3B). Forty-eight hours after infestation, we determined the wilted area of the tomato leaves. When the WT strain was in-phase with the plants, infection severity was greatest at dawn (Host-ZT0 and Pathogen-ZT0) (Fig. 3C). However, when the fungal phase was reversed, the peak of severe symptoms shifted to dusk (Host-ZT12 and Pathogen-ZT0) (Fig. 3D). These results suggest that *F. oxysporum* pathogenicity exhibits diurnal variation, with virulence peaking at Pathogen-ZT0.

To eliminate potential effects of light on these observations, we performed similar experiments with plants kept in DD postinfection (fig. S4A). Wilt severity increased in the dark, and diurnal differences persisted under DD conditions. Severe wilt was also observed when plants were infected with an *F. oxysporum* strain transitioned from dark to light (Pathogen-ZT0) (fig. S4, B and C). Because only the phase of *F. oxysporum* was altered during the infection process, the observed variation in infection severity, which was absent in clock mutants, is due to circadian clock–regulated fungal virulence.

Circadian gene expression in *F. oxysporum*

To investigate the relationship between virulence and the circadian clock in *F. oxysporum*, we conducted time-series transcriptomic analyses under free-running conditions. A key hallmark of circadian rhythms is the periodic expression of genes with a cycle of approximately 24 hours (±2 hours) in the absence of environmental cues (*5*). Using the periodicity-detecting algorithm eJTK_CYCLE

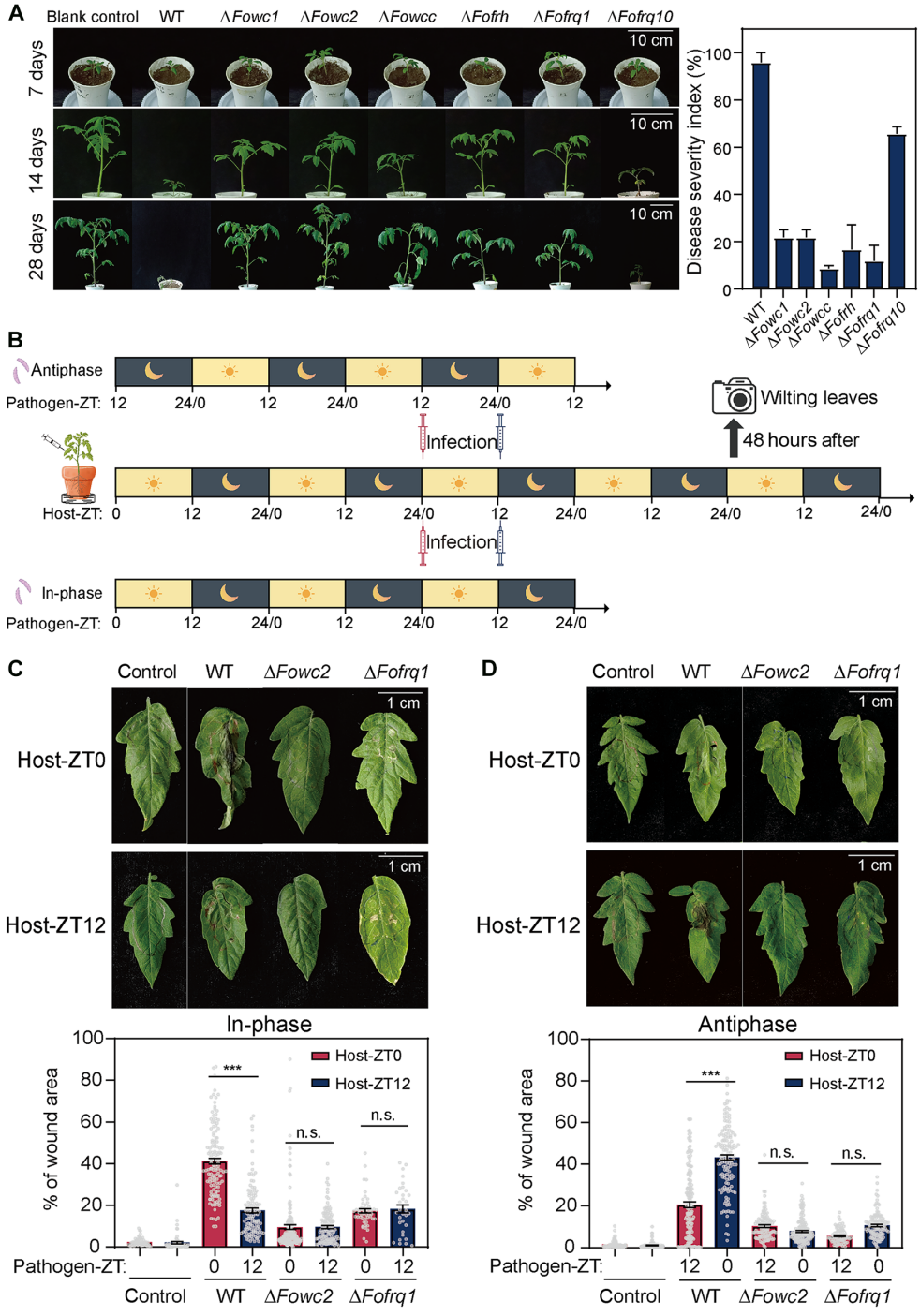

Fig. 3. The *F. oxysporum* circadian clock controls infection of tomato plants. (**A**) Pathogenicity of the WT and circadian clock mutants was examined. The roots of tomato seedlings were slightly wounded and immersed in a suspension of 5×10^6 conidia/ml of *F. oxysporum* at Host-ZT12. Infected seedlings were grown in the greenhouse at approximately 28°C, and DSI was calculated from 7 to 30 days postinoculation. Twelve plants were used for each treatment, and the experiments were conducted three times for each mutant. Photographs of representative infected tomato plants at 7, 14, and 28 days postinfection are shown. (**B**) Workflow to characterize the effects of the circadian clock of *F. oxysporum* on infection. Tomato seedlings were cultured under LL:DD (12:12) until they reached 30 days of age. Fungal strains were cultured in the same (in-phase) or opposite (antiphase) LD phase as the plants for 7 days. Plant leaves were infiltrated with fungi (as indicated by the red and black syringes) at alternating light and dark times (Host-ZT0 or Host-ZT12), and photographs were taken after 48 hours to document wilting (as indicated by the black camera). (**C** and **D**) WT and circadian clock mutant *F. oxysporum* strains were cultured on PDA plates for 7 days under (C) LD conditions (i.e., in-phase with the plants) or (D) DL conditions (i.e., antiphase with the plants). Tomato leaves were infiltrated with a suspension of 1×10^7 conidia/ml of *F. oxysporum* at Host-ZT0 or Host-ZT12 (the time points of light/dark transition), and then the plants were incubated in LD for 48 hours. Top: Photographs of representative leaves. Bottom: Quantification of lesion spread performed on at least 120 independent virulence assays. Error bars indicate SEMs. A Student's *t* test was conducted to determine statistical significance. ***$P < 0.001$; not significant (n.s.), $P \geq 0.05$.

(*45*), we identified 993 rhythmic genes oscillating on a 24-hour cycle (Fig. 4A and table S1). This substantial number of rhythmic genes provides further evidence for the presence of a functional circadian clock in *F. oxysporum*. Annotation of these rhythmic genes using the Kyoto Encyclopedia of Genes and Genomes (KEGG) database revealed that they are predominantly associated with transcription factors and metabolic components (Fig. 4B). Gene Ontology (GO) analysis showed that these genes are highly enriched in categories such as transcription factor activity, nucleus, and nucleoside biosynthetic processes (fig. S5A).

We then compared the differentially expressed genes (DEGs) between the WT strain and the Δ*Fowcc* mutant at DD24, the time point corresponding to peak *frq* expression. This comparison identified 972 genes that were down-regulated and 548 genes that were up-regulated in the Δ*Fowcc* mutant relative to the WT strain (Fig. 4C). KEGG analysis indicated that down-regulated genes were enriched in transcription factors and metabolic pathways (Fig. 4D), while up-regulated genes were associated with chaperones and metabolic processes (fig. S5B). GO analysis further confirmed the enrichment of categories such as transcription factor activity, ion binding, and

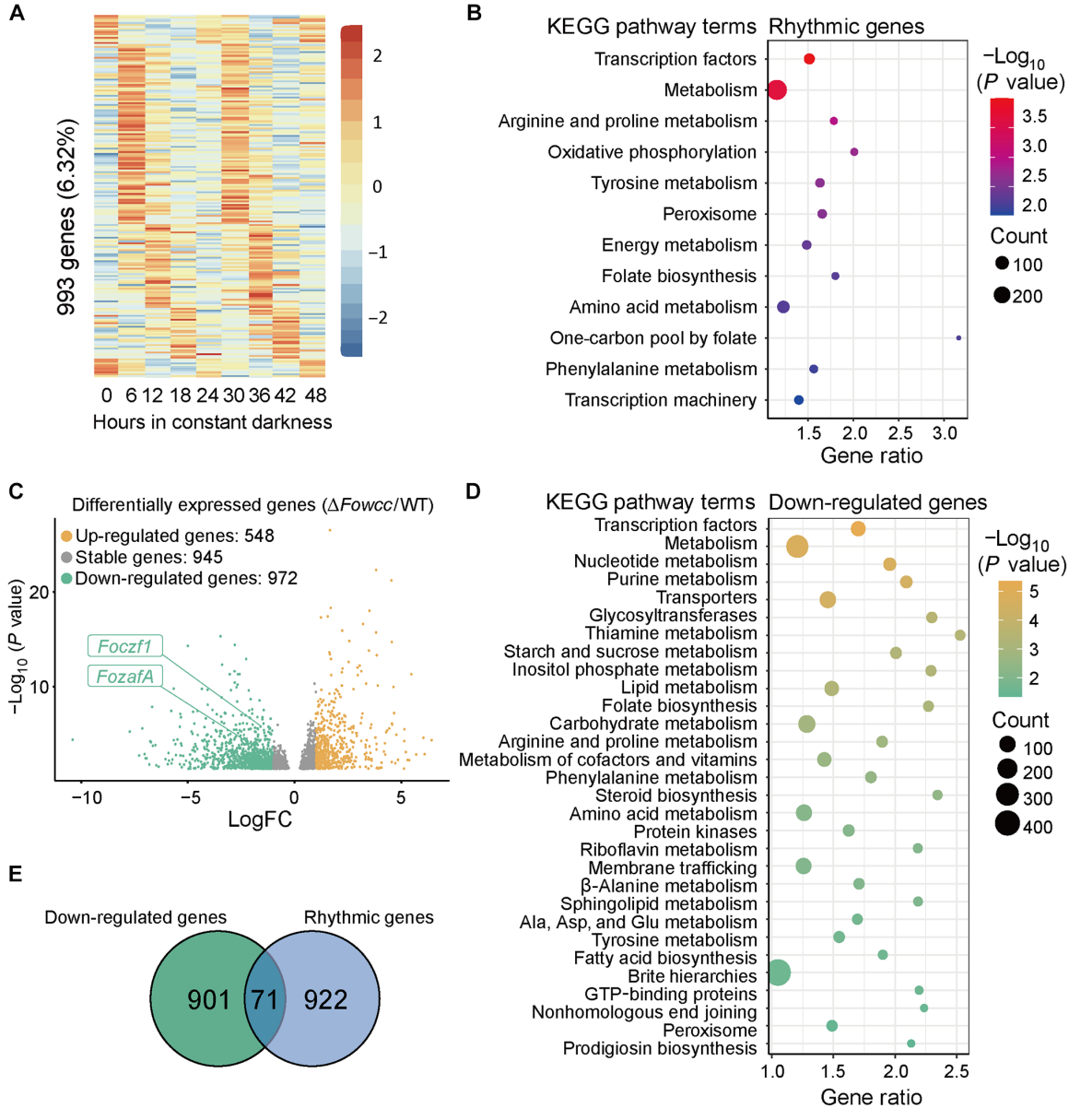

Fig. 4. Rhythmic expression of transcription factors is a major output of the *F. oxysporum* circadian clock. (**A**) Heatmap of gene expression by the WT strain of *F. oxysporum* over time in DD. Rhythmic genes were identified using eJTK_CYCLE. Each vertical line represents a time point, with gene expression displayed horizontally. Expression values were mean-normalized for each gene and are represented as a *z* score of SDs from the mean. (**B**) KEGG classification analysis of the rhythmic genes. (**C**) Volcano plot of differentially expressed genes (DEGs) in *F. oxysporum* between WT and Δ*Fowcc* at DD24. (**D**) KEGG classification analysis of down-regulated genes in the Δ*Fowcc* mutant compared to the WT strain. (**E**) Venn diagram of overlapping gene counts between down-regulated genes in the Δ*Fowcc* mutant compared to the WT strain and rhythmic genes in the WT strain. FC, fold change; GTP, guanosine triphosphate.

metabolism among these DEGs (fig. S5, C and D). Last, a comparison of overlapping genes revealed that 71 down-regulated genes and 29 up-regulated genes were rhythmically expressed (Fig. 4E and fig. S5E). These findings suggest that these genes may be direct targets of WCC, the positive regulator of the circadian negative feedback loop.

Among the 71 down-regulated genes that overlap with rhythmic genes, there is a notable enrichment for transcription factor genes, including nine rhythmic transcription factors (table S2). Of these nine transcription factors, FoZafA (FOXG_00370) and FoCzf1 (FOXG_00578) have been reported as critical for virulence in *F. oxysporum* (*46*), as indicated in Fig. 4C. This suggests that FoZafA and FoCzf1 may serve as critical clock-controlled pathogenicity factors involved in fungal pathogenesis and the host-pathogen interaction.

The rhythmicity of transcriptome has been extensively examined in *N. crassa* (*47*–*49*). Using blast analyses, we identified the homologs of *N. crassa* rhythmic genes (*47*) in *F. oxysporum* (table S3). There are 179 genes in *F. oxysporum* that overlap with the rhythmic genes in *N.crassa* and are enriched in zinc ion binding, DNA binding transcription factors, and transition metal ion binding (fig. S5F and table S3). We also identified the homologs of *N. crassa* WC-2 target genes (*47*, *50*) in *F. oxysporum* and found that 18 genes were categorized as rhythmic in both *N. crassa* and *F. oxysporum* (fig. S5F), including the homologous gene of *FozafA* in *N. crassa* (table S3), suggesting a conserved regulation of ZafA homologs by circadian clocks in fungi.

Circadian clock of *F. oxysporum* regulates zinc starvation response

Fungal pathogens must overcome the host's nutritional immunity, which restricts their access to metals and induces metal stress conditions (*51*). Zinc is one of these essential metals, playing a critical role in fungal virulence. FoZafA regulates zinc homeostasis and mediates the adaptive response to zinc starvation in pathogenic fungi (*52*, *53*). Reverse transcription quantitative polymerase chain reaction (RT-qPCR) analysis confirmed reduced transcription and an impaired circadian rhythm of *FozafA* in the Δ*Fowc2* mutant (Fig. 5A).

To further explore its role, we generated a Δ*FozafA* mutant, which exhibited a slower growth rate and dramatically reduced virulence toward tomato plants compared to the WT strain (Fig. 5, B and C). To assess whether FoZafA-mediated zinc homeostasis influences the altered virulence of circadian clock mutants, we evaluated the response of Δ*Fowcc* and Δ*Fofrq1* strains to zinc starvation. The expression levels of *FozafA* and *FozrfB*—the latter encoding a high-affinity zinc transporter regulated by FoZafA—were substantially reduced in the circadian mutants (Fig. 5, D and E). Consistent with this, the circadian clock mutants exhibited impaired reproduction under zinc starvation, with significantly reduced critical spore production (Fig. 5F). This finding suggests that the circadian clock plays a crucial role in the adaptation of *F. oxysporum* to zinc starvation. Collectively, these results highlight the importance of the clock-regulated virulence factor FoZafA in facilitating *F. oxysporum*'s adaptation to zinc homeostasis during infection of the tomato host.

Circadian clock–controlled secondary metabolites contribute to *F. oxysporum* pathogenicity

Fungal invasion of plants relies heavily on the secretion of phytotoxins generated through secondary metabolism (*51*). To determine whether secondary metabolites are involved in the circadian clock–regulated infection process, we harvested secondary metabolite extracts from WT and Δ*Fowcc* strains. These extracts, applied at a concentration of 50 μg/ml, were sprayed onto tomato plant leaves. Within 48 hours, plants treated with WT strain extracts exhibited wilting, while those treated with Δ*Fowcc* mutant extracts showed no wilting (Fig. 6A). This suggests that the circadian clock may regulate secondary metabolism by transmitting temporal signals through a hierarchical transcriptional regulatory network (*52*).

One such transcription factor, FoCzf1 (FOXG_00578), which activates the biosynthesis of the secondary metabolite fusaric acid (*53*), was found to display rhythmic expression (tables S1 and S2). As confirmed by RT-qPCR experiments, the rhythmic expression of *Foczf1* is dependent on FoWC2 (Fig. 6B), consistent with RNA sequencing (RNA-seq) data (Fig. 4, C and E), indicating its regulation by the circadian clock. Fusaric acid is a crucial phytotoxin that contributes to the virulence of *F. oxysporum* (*54*). To investigate whether the circadian clock regulates fusaric acid production, we performed high-performance liquid chromatography (HPLC) and mass spectrometry (MS) analyses on extracts from circadian clock mutants and their complementation strains. As expected, fusaric acid was undetectable in the Δ*Foczf1* strain (Fig. 6, C and D). Moreover, its production was dramatically reduced in the Δ*Fowcc* strain compared to the WT strain (Fig. 6, C and D). Complementation of each mutant with the corresponding gene restored fusaric acid production.

Genome annotation of *F. oxysporum* identified 50 secondary metabolite biosynthetic gene clusters, including those required for fusaric acid biosynthesis (table S2). RT-qPCR confirmed that the expression of fusaric acid biosynthetic genes was markedly reduced in the Δ*Foczf1*, Δ*Fowcc*, and Δ*Fofrq1* mutants (Fig. 7, A to C). Deletion of *Foczf1* also resulted in reduced growth rates and decreased pathogenicity toward tomato plants (Fig. 7, D and E). These findings demonstrate that fusaric acid, regulated by the clock-controlled transcription factor FoCzf1, is a major metabolite contributing to changes in *F. oxysporum* virulence. Overall, our study suggests that the circadian clock serves as a critical command system in *F. oxysporum*, orchestrating strategies for host invasion (Fig. 7F). Clock-controlled transcription factors act as key regulators, enabling the pathogen to adapt to host-induced stress and produce toxic metabolites through secondary metabolism. These sophisticated, clock-driven mechanisms empower *F. oxysporum* to bypass host defenses and infect at the optimal time.

DISCUSSION

In this study, we demonstrated the existence of a functional circadian clock in *F. oxysporum*, a soilborne organism that lacks an overtly rhythmic phenotype. In its core oscillator, the FoWC1-FoWC2 complex acts as a positive regulator to activate *Fofrq1* transcription (Fig. 2A), while the FoFRQ1-FoFRH complex functions as the negative regulator to repress FoWCC activity, forming a negative feedback loop (Fig. 2F). The expression of *Fowcc* was significantly reduced in the Δ*Fofrq1* mutant (Fig. 2E), indicating a positive regulation of *Fowcc* expression by FoFRQ1. This is similar to the positive feedback loop involving FRQ and WCC previously described in *N. crassa* (*7*, *42*). In the WT strain, the rhythmic activity of FoWCC governs the rhythm of genome-wide gene transcription. In the Δ*Fowcc* or Δ*Fofrq1* mutants, the loss or reduction of FoWCC disrupts circadian gene expression, resulting in impaired virulence. The reduced pathogenicity of circadian clock gene mutants, along with the diurnal variations in infection outcomes, indicates that the circadian clock is critical for fungal virulence in *F. oxysporum*.

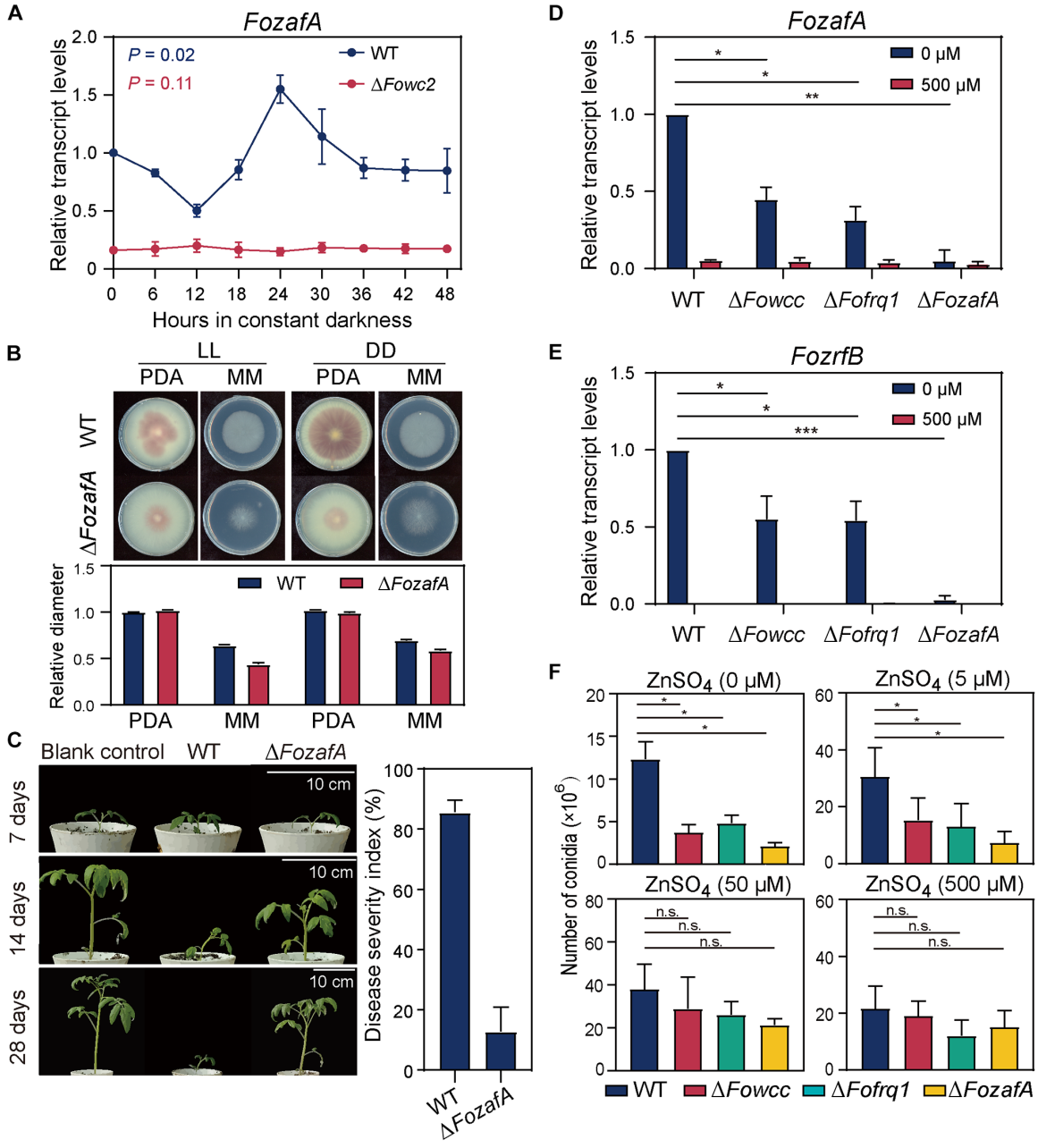

Fig. 5. The *F. oxysporum* circadian clock regulates the response to zinc starvation through rhythmic expression of FoZafA. (**A**) RT-qPCR analyses of *FozafA* mRNA in WT and Δ*Fowc2* mutant as a function of time in DD. (**B**) Photographs of WT and Δ*FozafA* mutant incubated on PDA or minimal medium (MM) to evaluate growth phenotype. (**C**) Photographs of plants infected with WT and Δ*FozafA* mutant. (**D** and **E**) RT-qPCR analyses of (D) *FozafA* and (E) *FozrfB* during zinc starvation in WT and circadian clock mutants. (**F**) Spore production by WT and circadian clock mutants under varying $ZnSO_4$ concentrations over 5 days. Error bars indicate SDs ($n \geq 3$). A Student's *t* test was conducted to determine statistical significance. $^*P < 0.05$; $^{**}P < 0.01$; $^{***}P < 0.001$; n.s., $P \geq 0.05$.

Transcriptome analysis revealed that the circadian clock governs the rhythmic expression of genes, particularly those enriched in transcription factors and metabolism, with partial overlap with reported pathogenic factors (Fig. 4). This regulation enables *F. oxysporum* to adapt to the host environment, such as by mitigating zinc starvation stress and enhancing production of the phytotoxin fusaric acid (Figs. 5 and 6). Thus, the circadian clock coordinates rhythmic transcription factors, facilitating extensive downstream transcriptional regulation. This interlocking regulatory network is essential for fungal development, stress responses, secondary metabolism, and other critical functions (Fig. 7F).

Most eukaryotic and some prokaryotic organisms, including pathogenic microbes, have circadian clocks that aid in environmental adaptation through conserved mechanisms (*2*, *5*). In pathogens, circadian clocks have evolved specific functions in response to natural and host-imposed selective pressures. In fungal pathogens such as *A. flavus* and *B. cinerea*, circadian clocks regulate development or virulence to adapt to adverse environmental

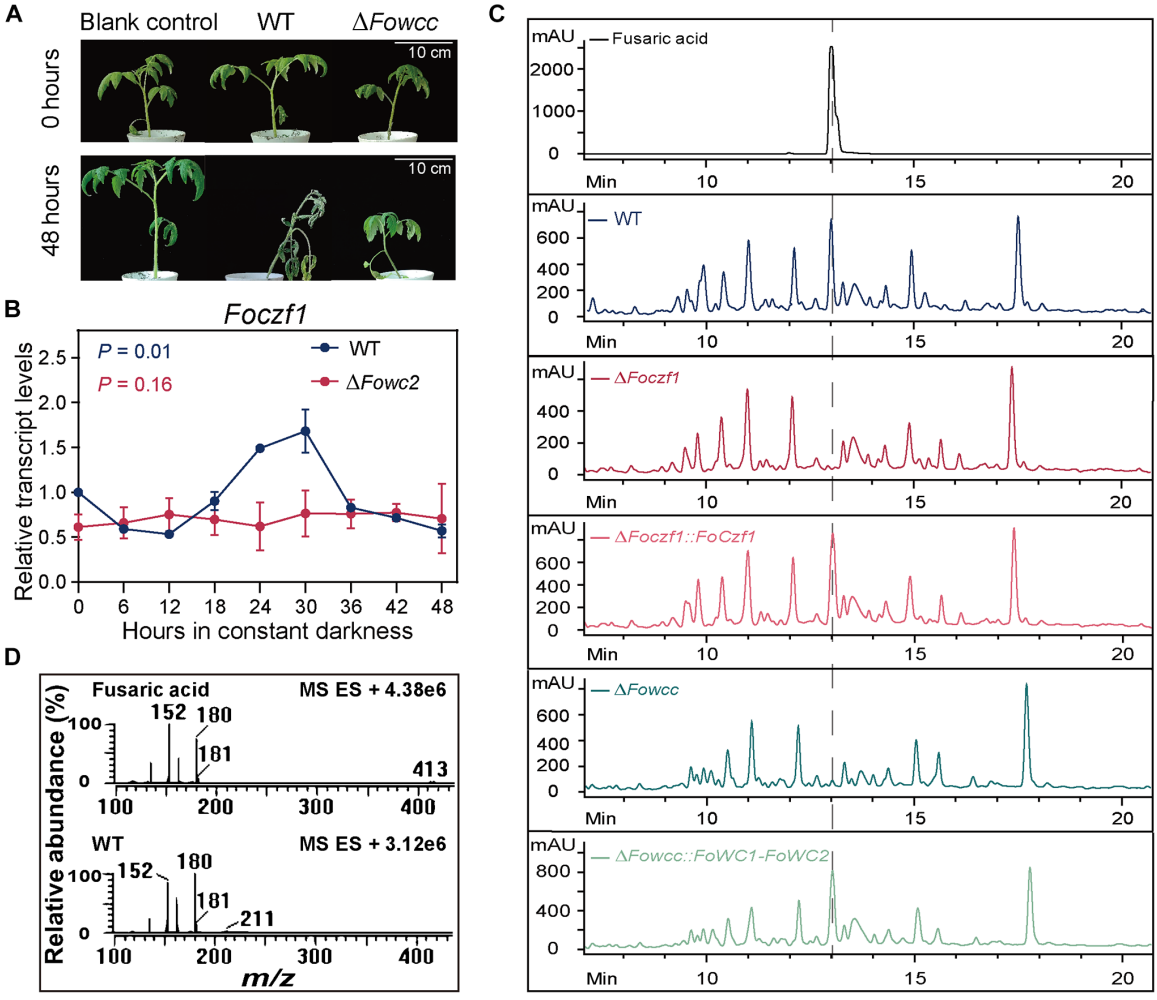

Fig. 6. The *F. oxysporum* circadian clock regulates secondary metabolite fusaric acid through the virulence factor FoCzf1. (**A**) Toxicity analysis of crude extracts from WT and Δ*Fowcc*. Secondary metabolic extracts from WT and Δ*Fowcc* strains were collected and sprayed on the leaves of tomato plants. Experiments were performed three times for each mutant, and representative photographs were shown. (**B**) RT-qPCR analysis of *Foczf1* mRNA in WT and *Fowc2* strains as a function of time in DD. (**C**) High-performance liquid chromatography (HPLC) analysis (λ =230 nm) of fusaric acid in the WT strain, Δ*Foczf1*, Δ*Fowcc* mutants, and Δ*Foczf1::FoCzf1* and Δ*Fowcc::FoWC1-FoWC2* complementation strains. The indicated strains were cultivated for 7 days under high nitrogen conditions, and the cultures were extracted with ethyl acetate for chemical analysis. mAU, milli-absorbance units. (**D**) Mass spectrometry (MS) analysis of fusaric acid standard and metabolites produced by the WT strain, highlighting the peaks of fusaric acid. ES+, positive electrospray; *m/z*, mass/charge ratio.

conditions (*16*, *17*). FRQ is a well-studied core circadian clock protein in filamentous fungi (*17*, *18*, *20*, *40*, *55*). Most fungi have one or two FRQ homologs; however, *F. oxysporum* contains an exceptional 10 FRQ homologs (Fig. 1 and fig. S1) (*37*). This multiplicity of FRQ homologs likely allows *F. oxysporum* to adapt to fluctuating environments during prolonged interactions with diverse hosts. Although *F. oxysporum* does not reproduce sexually, it enhances genetic diversity through genetic recombination and horizontal gene transfer (*23*). More than half of the FoFRQ genes are located on accessory genomes, such as chromosome 15, and were likely acquired through horizontal gene transfer (Fig. 1B). This mechanism is further supported by the variability in the number of FoFRQ genes across different forma specialis of *F. oxysporum* (fig. S1A).

The importance of the circadian clock in host-pathogen interactions was suggested decades ago through observations of diurnal variations in host immune responses to lethal infections (*33*, *56*, *57*). However, the precise role of circadian clocks in coordinating interactions between hosts and their microbial communities remains unclear. The host circadian clock regulates the host immune system, enabling rapid elimination of pathogens (*34*, *58*, *59*). For example, the circadian clock in mice modulates the immune response to the bacterial pathogen *Salmonella typhimurium* (*33*, *60*), while the clock component CCA1 in *Arabidopsis* allows the plant to anticipate infections caused by the fungal pathogen *Hyaloperonospora arabidopsidis* at dawn (*61*, *62*). Pathogen circadian clocks can also coordinate development and infection processes (*59*). Microbial pathogens exhibit timed virulence, exploiting host defenses to their advantage as a classic strategy to evade host resistance (*63*). Studies have shown that circadian clock elements can affect fungal virulence. For instance, the absence of core circadian regulator WCC or FRQ reduces virulence in several fungi (*17*, *55*, *64*–*67*). However, the virulence

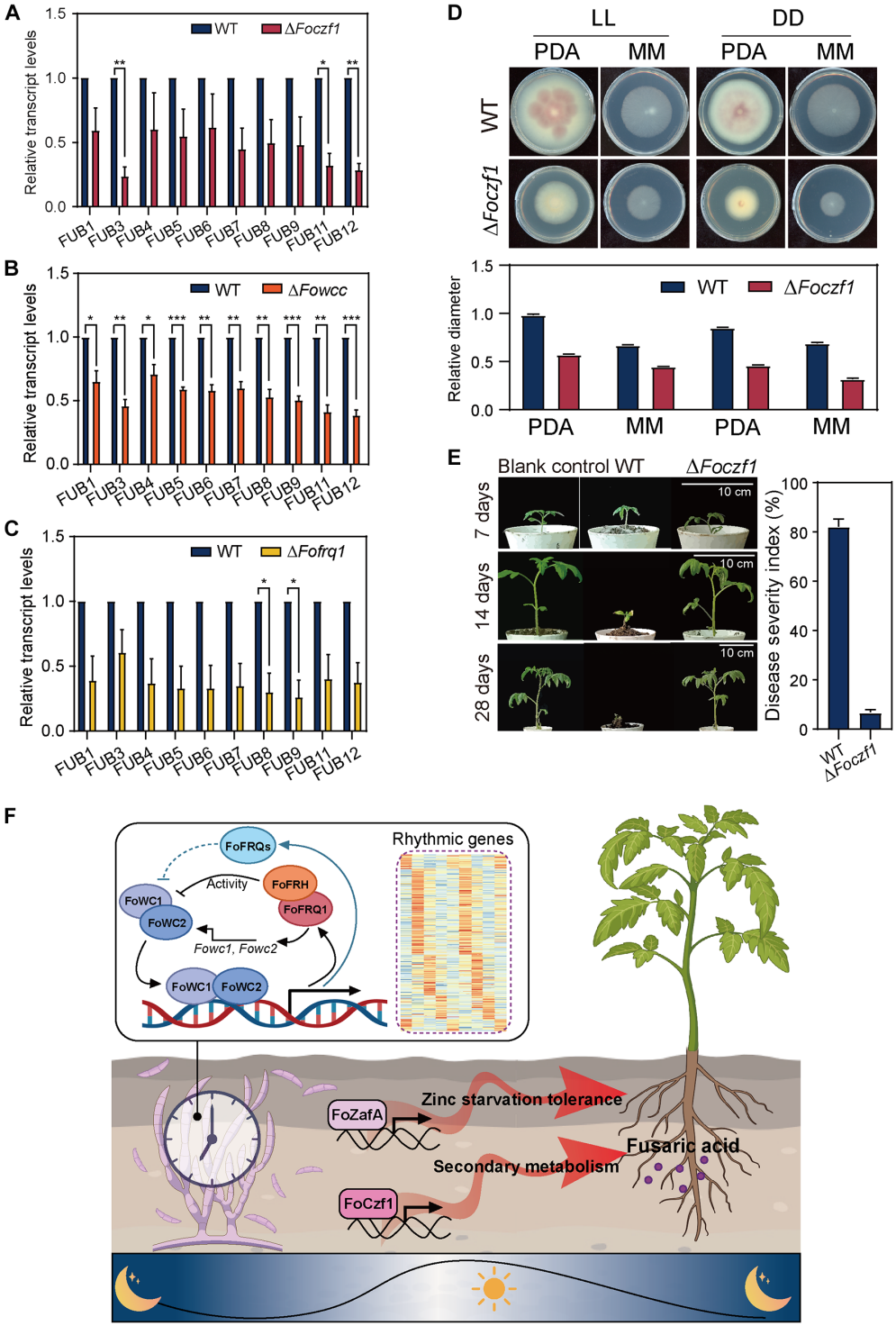

Fig. 7. The *F. oxysporum* circadian clock is important for fungal virulence by regulating fusaric acid biosynthesis through FoCzf1. (**A** to **C**) Levels of fusaric acid biosynthetic genes (FUB) determined by RT-qPCR in WT strain and Δ*Foczf1*, Δ*Fowcc*, and Δ*Fofrq1* mutants in DD. Error bars indicate SDs ($n \geq 3$). (**D**) Photographs of WT and Δ*Foczf1* mutant incubated on PDA or MM to evaluate growth phenotype. (**E**) Photographs of plants infected with WT or Δ*Foczf1* mutant. A Student's *t* test was conducted to determine statistical significance. $^{*}P < 0.05$, $^{**}P < 0.01$, and $^{***}P < 0.001$. (**F**) A model to explain how the endogenic circadian clock in *F. oxysporum* contributes to virulence and infection. Interconnected feedback loops, both positive and negative, are formed by FoWC1-FoWC2 and FoFRQ1-FoFRH. Rhythmic genes governed by the circadian clock dramatically influence *F. oxysporum* metabolism (both basic and secondary). The circadian clock acts as a command center in *F. oxysporum*, orchestrating the host invasion through clock-controlled virulence factors. The adaptation of *F. oxysporum* to stress within the host and the production of phytotoxin via secondary metabolism are regulated by the circadian clock.

factors controlled by the circadian clock in these fungi remain unknown. On the other hand, in some pathogens, such as *V. dahliae* and *M. robertsii*, circadian clock components are not essential for virulence (*19*, *20*, *40*).

In this study, we demonstrated the critical role of the circadian clock in regulating *F. oxysporum* virulence and its interaction with tomato hosts. The circadian clock governs the rhythmic expression of transcription factors, such as FoZafA and FoCzf1, which are vital for the fungal adaptation to zinc starvation stress in the host and the production of the secondary toxin fusaric acid (Figs. 4 and 5). Both FoZafA and FoCzf1 are transcription factors containing C_2H_2 zinc finger domains. FoZafA is an ortholog of Zap1 in the budding yeast *Saccharomyces cerevisiae*, where it acts as a central regulator of zinc homeostasis (*68*). Orthologs of FoZafA are also present in other pathogenic fungi, including *Aspergillus fumigatus* and *Candida albicans*, where they are also important for virulence (*68*–*70*). Similarly, FoCzf1 is widely conserved across fungi, and loss of function has been associated with reduced virulence in pathogens such as *Fusarium graminearum* and *Magnaporthe oryzae* (*46*, *53*). These findings suggest that ZafA and Czf1 homologs in other fungi may also play critical roles in clock-controlled fungal pathogenesis.

Pathogenic fungi use various effectors, such as secreted proteins, nucleic acids, and secondary metabolites, to suppress the plant host immune system and promote infection (*52*, *71*–*75*). While secondary metabolites are not essential for normal growth, they may provide a selective advantage in specific environments (*52*, *76*). Soilborne pathogens are known to invade plants in the rhizosphere, a complex environment with various microorganisms (*77*, *78*), where secondary metabolites play crucial roles in multiorganism interactions and ecological niche colonization (*75*). Circadian clocks transmit temporal signals downstream through extensive transcriptional regulatory networks that have the potential to orchestrate global gene regulation. A study in *T. atroviride* demonstrated that TaFRQ acts as a general repressor of secondary metabolism, mediating fungal-fungal interactions (*18*). However, the interaction between fungal circadian clocks and secondary metabolism still needs to be systematically explored in different fungi. Here, we show that secondary metabolism in *F. oxysporum* is regulated by the circadian clock, which is critical for fungal virulence and its interaction with the host. Fusaric acid, a well-known phytotoxin produced by *F. oxysporum*, is toxic to the tomato host and influences the plant's rhizosphere microbiome (*53*, *54*, *79*). Specifically, the transcription factor FoCzf1 activates the gene clusters responsible for fusaric acid synthesis and is itself regulated by the circadian clock (Figs. 6 and 7). Our results indicate that the circadian clock in *F. oxysporum* establishes molecular connections between fungal secondary metabolism and plant host immunity by regulating the virulence factor FoCzf1 and fusaric acid production.

In summary, our findings underscore the importance of the endogenous circadian clock in *F. oxysporum* pathogenesis and host invasion. Given the circadian clock's role in cross-kingdom communication, which enhances sustainable agriculture, the development of biofungicides based on clock-controlled host-pathogen interactions presents a promising strategy for managing soilborne pathogens (*32*, *80*).

MATERIALS AND METHODS

Strains and culture conditions

The strain of *F. oxysporum* f. sp. *lycopersici*, originally isolated from Tomato (*Solanum lycopersicum*) (*81*), was used as the WT strain for genetic modifications. Δ*Fowc1*, Δ*Fowc2*, Δ*Fofrq1*, Δ*Fofrq10*, Δ*Fofrh*, Δ*FozafA*, and Δ*Foczf1* strains were generated using homologous recombination with the hygromycin resistance gene. To generate the Δ*Fowcc* strain using homologous recombination, *Fowc2* was replaced with a hygromycin resistance gene, and *Fowc1* was replaced with a neomycin resistance gene. Constructs with the *cfp* promoter–driven expression of Myc-FoFRQ1 or Myc-FoWC2 strain were generated by random insertion with the neomycin resistance gene. Cfp-Flag-FoFRH was introduced into the cfp-Myc-FoFRQ1 strain and screened with hygromycin B to obtain Myc-FoFRQ1; Flag-FoFRH strain. Cfp-Flag-FoWC1 was introduced into the cfp-Myc-FoWC2 strain and screened with hygromycin B to obtain Myc.FoWC2; Flag.FoWC1 strain. Complementation strains Δ*Fowcc*-Myc-FoWC2, Flag-FoWC1, Δ*Fofrh*-Myc-FoFRH, and Δ*Foczf*-Myc-FoCzf1 were generated by random insertion of the target gene into the corresponding knockout mutant with neomycin selection. *F. oxysporum* strains were cultivated in Potato Dextrose Agar (PDA) medium at 28°C using an incubator or grown in Potato Dextrose Broth (PDB) medium using incubator shakers in a 12:12-hour LD cycle.

Protoplast preparation and transformation of *F. oxysporum*

F. oxysporum transformations were carried out using protoplast-mediated transformation. Briefly, 1×10^8 of conidia from *F. oxysporum* were inoculated into 50 ml of PDB medium and cultivated at 28°C for 4 to 6 hours with shaking at 200 rpm. The germlings were harvested with a centrifuge of 1000*g* at 4°C for 15 min, washed three times with 0.7 M NaCl, and then digested with disease (10 mg/ml), lysing enzyme from *Trichoderma harzianum* (10 mg/ml), and cellulase from *Trichoderma longibrachiatum* (15 mg/ml) at 30°C for 1 and 2 hours with shaking at 100 rpm. The protoplasts were collected by centrifugation of 1000*g* at 4°C for 5 min and washed twice with Sobital, Tris-HCl, $CaCl_2$ (STC) buffer [1.2 M sorbitol, 10 mM tris-HCl (pH 8.0), and 50 mM $CaCl_2$]. Last, the protoplasts were diluted in storage buffer [STC:SPTC:dimethyl sulfoxide = 8:2:0.1 (v/v); SPTC buffer: 0.8 M sorbitol, 50 mM tris-HCl (pH 8.0), 50 mM $CaCl_2$, and 40% polyethylene glycol, molecular weight 8000 (PEG-8000)] at a final concentration of 1×10^8 protoplasts/ml.

For transformation, 1 to 10 mg of DNA in 100 μl of STC buffer was mixed with 100 μl of protoplasts, and then 50 μl of 30% PEG-8000 (v/v) was added and incubated at room temperature for 20 min. After incubation, 2 ml of 30% PEG-8000 (v/v) was added and incubated for 5 min. STC buffer of 4 ml was added before mixing thoroughly. The mixture was dissolved in molten regeneration medium [0.1% yeast extract (w/v), 0.1% casein-enzyme hydrolysate (w/v), 0.8 M sucrose, and 1.5% agar (w/v)] at 50°C and poured into petri dishes. The transformants were cultivated at 28°C for 12 hours, and overlay regeneration medium with selective reagent was added to the plate for further screening.

Luciferase reporter assay

The luciferase reporter assay was performed as reported previously (*82*). The luciferase gene was inserted at the end of the *Fofrq1* gene in the WT and Δ*Fowc1* strains by homologous recombination with hygromycin B selection. Conidial suspension was placed on autoclaved Czapek Dox medium, replaced sucrose with 1% sorbose (0.3% sodium nitrate, 0.1% dipotassium phosphate, 0.05% magnesium sulfate, 0.05% potassium chloride, 0.001% ferrous sulfate, and 1.5% agar (pH 7.2)] with 50 μM firefly luciferin, and grown in constant light overnight. The cultures were then transferred to DD, and

luminescence was recorded in real time using a LumiCycle for 5 days in DD. The data were then normalized with LumiCycle Analysis software by subtracting the baseline luciferase signal, which increases as the strain grows.

RNA extraction and RT-qPCR analysis

Strain cultures were frozen in liquid nitrogen and ground to powder. Total RNA was extracted and purified using an Ultrapure RNA Kit [CoWin Biosciences (CWBIO), CW0581S] according to the manufacturer's instructions. A FastQuant RT Kit with gDNase (Vazyme, CW0581S) was used for first-strand cDNA synthesis. The RT-qPCR was conducted using power SYBR qPCR premix reagents (CWBIO, CW0957H) in a CFX96 Touch Real-time PCR detection system (Bio-Rad), and relative transcript levels were calculated as fold changes and normalized to the housekeeping gene *actin* (FOXG_01569) using the comparative Ct method. Primers used for RT-qPCR are listed in table S4.

Protein analysis

Protein extraction, quantification, and Western blot analyses were conducted as previously described (*83*, *84*). Briefly, tissue was ground in liquid nitrogen using a mortar and pestle and suspended in ice-cold extraction buffer [50 mM Hepes (pH 7.4), 137 mM NaCl, and 10% glycerol] containing protease inhibitors [pepstatin A (1 mg/ml), leupeptin (1 mg/ml), and 1 mM phenylmethylsulfonyl fluoride]. Following centrifugation, protein concentration was assessed using a protein assay dye reagent (Bio-Rad, 5000205). For Western blot analyses, equal amounts of total protein (40 mg) were loaded into each lane of 7.5 or 10% SDS–polyacrylamide gel electrophoresis gels with an acrylamide-to-bisacrylamide ratio of 37.5:1. After electrophoresis, proteins were transferred to polyvinylidene difluoride membranes, and Western blot analyses using anti-Myc (TransGen, HT101), anti-Flag (Sigma-Aldrich, F1804), and anti-luciferase (Sigma-Aldrich, L2164) antibodies were performed. Western blot signals were detected using x-ray films and scanned for quantification.

Co-IP analysis

Co-IP analysis was performed as previously described (*83*). Briefly, proteins were extracted as described above. For each IP reaction, 2 mg of protein and 2 μl of anti-Myc antibody were used. After incubation with anti-Myc antibody for 3 hours, 40 μl of GammaBind G Sepharose beads (GE Healthcare, 17061801) was added, and samples were incubated for 1 hour. Immunoprecipitated proteins were washed three times using extraction buffer before Western blot analysis with anti-Myc and anti-Flag antibodies.

ChIP-qPCR

Chromatin immunoprecipitation (ChIP) assays were performed as previously described (*83*–*85*). Briefly, the germinating conidia of different strains were cultured in yeast extract, peptone, and dextrose medium [glucose (20 g/liter), peptone (20 g/liter), and yeast extract(10 g/liter)] with shaking at 150 rpm at 25°C. Before harvest, 1% formaldehyde (37%) was added directly to the liquid culture to cross-link the proteins with the chromatin, followed by a 15-min incubation. To halt the cross-linking, 125 mM glycine (pH 7.5) was added, and the mixture was incubated for an additional 5 min. The culture was washed several times with 1× phosphate-buffered saline and harvested after treatment. IP was performed using 2 mg of protein and 1 μl of anti-Myc antibody along with GammaBind G Sepharose beads overnight at 4°C. After separation, beads were washed sequentially with low-salt wash buffer [150 mM NaCl, 0.2% SDS, 20 mM tris-HCl (pH 8.0), 2 mM EDTA, and 0.5% Triton X-100], high-salt wash buffer [500 mM NaCl, 2 mM EDTA, 20 mM tris-HCl (pH 8.0), 0.2% SDS, and 0.5% Triton X-100], LiCl wash buffer [0.25 M LiCl, 1% NP-40, 1% sodium deoxycholate, 1 mM EDTA, and 10 mM tris-HCl (pH 8.0)], and TE buffer. DNA bound to the beads was subsequently eluted and precipitated. ChIP-qPCR was independently repeated three times. Relative enrichment values were calculated by dividing the immunoprecipitated DNA by the input DNA and the internal control gene (actin). Primers used for ChIP-qPCR are listed in table S4.

Time course experiments

Strains were grown in incubators at 28°C. For circadian rhythm experiments under DD conditions, the WT strain and clock mutants were grown on PDA plates covered with cellophane under constant light conditions for 24 hours and then transferred to DD every 6 hours. After 48 hours, mycelium samples (obtained from independent PDA plates) were harvested. Protein or RNA isolation and RT-qPCR procedures were conducted.

Virulence assay

Before infection, *F. oxysporum* was grown in PDA under varying light conditions for 7 days at 28°C. Sterile tomato plants (cultivar: Zhongza9) for the virulence assays in roots were grown at 28°C until the two true leaves stage, receiving 12 hours of light each day. Subsequently, plant roots were inoculated with *F. oxysporum* conidia (5×10^6 spores/ml), obtained from PDA plates. Pathogenicity was assessed 4 weeks postinoculation in the greenhouse under 12:12-hour LD conditions. Disease indices were scored on a scale of 0 to 4: 0, no disease symptoms; 1, slight wilting on true or cotyledon leaves, but growth remained normal; 2, distinct necrotic plaques appeared on true or cotyledon leaves, with roots becoming diseased and growth delayed; 3, root necrosis and parts of the plant wilted or exhibited growth rigidity; 4, the entire plant wilted, and the plant was either dead or very small and wilted (*86*). DSI was calculated using the following formula: $\mathrm{DSI} = [\sum (\text{class} \times \text{number of plants in that class})/(4 \times \text{total number of assessed plants})] \times 100$. Each treatment consisted of three replicates, with 12 seedlings per replicate.

For leaf inoculation, *F. oxysporum* spores were harvested from the same plate at dawn or dusk, and conidial suspensions of 1×10^7 spores/ml were infiltrated into unwounded tomato leaves (1 month old). Infections were conducted at 9:00 (Host-ZT0) or 21:00 (Host-ZT12), in accordance with the photoperiod of the *F. oxysporum* growth chamber. All inoculated plants were maintained inside plastic boxes at 28°C in a humid environment, under LD or dark/light (DL) conditions for 48 hours, and then immediately analyzed (2 days post-noculation). Lesions on tomato leaves (at least 120 infected leaves per *F. oxysporum* strain and condition) were measured semiautomatically using ImageJ software with an external calibration scale. Because of the varying leaf sizes, the lesion area was calculated by measuring both the total and the infected areas of the leaf, with the total area representing 100%. Consequently, the measurements in the graphs are expressed as percentages.

RNA-seq analysis

RNA-seq data were analyzed as previously described (*83*). The reference genome of *F. oxysporum* f. sp. *lycopersici* 4287 was downloaded

from the following link: www.ncbi.nlm.nih.gov/datasets/genome/GCF_000149955.1/. Raw reads were filtered using SOAPnuke (v1.4.0) to obtain high-quality reads by removing low-quality reads with $Q < 15$. After trimming low-quality bases ($Q < 15$) and adaptor sequences, the resulting high-quality reads were aligned to the downloaded reference genome using HISAT2 (v2.1.0) and Bowtie2 (v2.2.5). The reads were assembled and normalized. Gene expression levels were quantified in terms of fragments per kilobase of exon per million fragments mapped (FPKM) using RSEM v1.2.8 (http://deweylab.biostat.wisc.edu/rsem/rsem-calculate-expression.html). Heatmaps were generated using FPKM values with the heatmap2 function of the R package (www.R.project.org/). DESeq2 was used to identify DEGs based on false discovery rate (FDR) adjusted $P \leq 0.05$, after Benjamini-Hochberg correction for multiple testing and absolute $\log_2$ fold change values of ≥1, with significance marked as "yes." Circadian rhythms were assessed through eJTK_cycle analysis (*45*). After Benjamini-Hochberg adjustments, any gene with a $P < 0.05$ was considered rhythmically expressed in this study. GO enrichment analysis was performed using Blast2GO 2.5.0, and KEGG enrichment was conducted using KOBAS 2.0. The two-tailed Fisher's exact test, based on the FDR cutoff of 0.05, was used as one of the justification conditions. Annotation of *F. oxysporum* genomic secondary metabolic synthesis gene clusters was completed using antiSMASH database version 4 (https://antismash-db.secondarymetabolites.org/).

HPLC-MS analysis of the secondary metabolites

F. oxysporum was cultivated for 7 days at 28°C on PDA medium. The strain spores were collected using sterile water and adjusted to 1×10^5 spores/ml. Fermentation was performed in 300 ml of PDB and incubated for 1 week at 28°C with shaking at 150 rpm. Using ultrasonication, the fermented broths were extracted with ethyl acetate, and the organic solvent was filtered and evaporated to dryness under vacuum to obtain the crude extract.

The crude extract of the WT strain and mutants was subjected to HPLC-MS analysis (Kromasil, 100-5-C8 column; 4.6 mm by 250 mm; 1.0 ml/min; ultraviolet detection at 230 nm), using a gradient flow of acetonitrile and water (0.3% acetic acid was added to the mobile phase) over 45 min. The retention time for the authentic standard fusaric acid was 13 min. The entire column flow was directed to the mass spectrometer. The operation of the chromatography and MS instruments, as well as the quantification of the eluting fusaric acid, was conducted using Agilent OpenLab software. All experiments were conducted using a Waters antibody drug conjugate. The mass spectrometer operated under the following parameters: polarity: electrospray, capillary: 2 kV; sampling cone: 40; source temperature: 100°C; desolvation temperature: 450°C; sample infusion flow rate: 30 μl/min; LockSpray infusion flow rate: 5 μl/min; and LockSpray capillary: 2.5 kV. Data were acquired with MassLynx v4.2 software. Uncertainties in mean determinations are expressed in terms of SD.

Quantification and statistical analyses

Quantification of Western blot data was performed using ImageJ software. All studies were performed on at least three independent experiments. Error bars are SDs for RT-qPCR, Western blot, and ChIP assays and SEMs for virulence assays. Statistical significance was determined by Student's *t* test.

Supplementary Materials

The PDF file includes:
Figs. S1 to S5
Images of uncropped Western blots
Legends for tables S1 to S4

Other Supplementary Material for this manuscript includes the following:
Tables S1 to S4

REFERENCES AND NOTES

1. C. H. Johnson, C. Zhao, Y. Xu, T. Mori, Timing the day: What makes bacterial clocks tick? *Nat. Rev. Microbiol.* **15**, 232–242 (2017).
2. D. Bell-Pedersen, V. M. Cassone, D. J. Earnest, S. S. Golden, P. E. Hardin, T. L. Thomas, M. J. Zoran, Circadian rhythms from multiple oscillators: Lessons from diverse organisms. *Nat. Rev. Genet.* **6**, 544–556 (2005).
3. J. S. Takahashi, Transcriptional architecture of the mammalian circadian clock. *Nat. Rev. Genet.* **18**, 164–179 (2017).
4. S. Panda, Circadian physiology of metabolism. *Science* **354**, 1008–1015 (2016).
5. J. C. Dunlap, J. J. Loros, Making time: Conservation of biological clocks from fungi to animals. *Microbiol Spectr* **5**, 10.1128/microbiolspec.FUNK-0039-2016 (2017).
6. S. K. Crosthwaite, J. C. Dunlap, J. J. Loros, *Neurospora wc-1* and *wc-2*: Transcription, photoresponses, and the origins of circadian rhythmicity. *Science* **276**, 763–769 (1997).
7. P. Cheng, Y. Yang, Y. Liu, Interlocked feedback loops contribute to the robustness of the *Neurospora* circadian clock. *Proc. Natl. Acad. Sci. U.S.A.* **98**, 7408–7413 (2001).
8. A. C. Froehlich, J. J. Loros, J. C. Dunlap, Rhythmic binding of a WHITE COLLAR-containing complex to the *frequency* promoter is inhibited by FREQUENCY. *Proc. Natl. Acad. Sci. U.S.A.* **100**, 5914–5919 (2003).
9. P. Cheng, Q. He, Q. He, L. Wang, Y. Liu, Regulation of the *Neurospora* circadian clock by an RNA helicase. *Genes Dev.* **19**, 234–241 (2005).
10. Q. He, J. Cha, Q. He, H. C. Lee, Y. Yang, Y. Liu, CKI and CKII mediate the FREQUENCY-dependent phosphorylation of the WHITE COLLAR complex to close the *Neurospora* circadian negative feedback loop. *Genes Dev.* **20**, 2552–2565 (2006).
11. T. Schafmeier, A. Haase, K. Káldi, J. Scholz, M. Fuchs, M. Brunner, Transcriptional feedback of circadian clock gene by phosphorylation-dependent inactivation of its transcription factor. *Cell* **122**, 235–246 (2005).
12. L. F. Larrondo, C. Olivares-Yanez, C. L. Baker, J. J. Loros, J. C. Dunlap, Decoupling circadian clock protein turnover from circadian period determination. *Science* **347**, 1257277 (2015).
13. X. Liu, A. Chen, A. Caicedo-Casso, G. Cui, M. Du, Q. He, S. Lim, H. J. Kim, C. I. Hong, Y. Liu, FRQ-CK1 interaction determines the period of circadian rhythms in *Neurospora*. *Nat. Commun.* **10**, 4352 (2019).
14. Q. He, P. Cheng, Y. H. Yang, Q. Y. He, H. T. Yu, Y. Liu, FWD1-mediated degradation of FREQUENCY in *Neurospora* establishes a conserved mechanism for circadian clock regulation. *EMBO J.* **22**, 4421–4430 (2003).
15. Y. Hu, X. Liu, Q. Lu, Y. Yang, Q. He, Y. Liu, X. Liu, FRQ-CK1 interaction underlies temperature compensation of the *Neurospora* circadian clock. *MBio* **12**, e0142521 (2021).
16. A. V. Greene, N. Keller, H. Haas, D. Bell-Pedersen, A circadian oscillator in *Aspergillus* spp. regulates daily development and gene expression. *Eukaryot. Cell* **2**, 231–237 (2003).
17. M. A. Hevia, P. Canessa, H. Muller-Esparza, L. F. Larrondo, A circadian oscillator in the fungus *Botrytis cinerea* regulates virulence when infecting *Arabidopsis thaliana*. *Proc. Natl. Acad. Sci. U.S.A.* **112**, 8744–8749 (2015).
18. M. Henriquez-Urrutia, R. Spanner, C. Olivares-Yanez, A. Seguel-Avello, R. Perez-Lara, H. Guillen-Alonso, R. Winkler, A. Herrera-Estrella, P. Canessa, L. F. Larrondo, Circadian oscillations in *Trichoderma atroviride* and the role of core clock components in secondary metabolism, development, and mycoparasitism against the phytopathogen *Botrytis cinerea*. *eLife* **11**, e71358 (2022).
19. E. Cascant-Lopez, S. K. Crosthwaite, L. J. Johnson, R. J. Harrison, No evidence that homologs of key circadian clock genes direct circadian programs of development or mRNA abundance in *Verticillium dahliae*. *Front. Microbiol.* **11**, 1977 (2020).
20. A. Nagel, M. Leonard, I. Maurus, J. Starke, K. Schmitt, O. Valerius, R. Harting, G. H. Braus, The Frq-Frh complex light-dependently delays Sfl1-induced microsclerotia formation in *Verticillium dahliae*. *J. Fungi.* **9**, 725 (2023).
21. S. Brody, Circadian rhythms in fungi: Structure/function/evolution of some clock components. *J. Biol. Rhythms* **34**, 364–379 (2019).
22. L. F. Larrondo, P. Canessa, The clock keeps on ticking: Emerging roles for circadian regulation in the control of fungal physiology and pathogenesis. *Curr. Top. Microbiol. Immunol.* **422**, 121–156 (2019).
23. L. J. Ma, D. M. Geiser, R. H. Proctor, A. P. Rooney, K. O'Donnell, F. Trail, D. M. Gardiner, J. M. Manners, K. Kazan, Fusarium pathogenomics. *Annu. Rev. Microbiol.* **67**, 399–416 (2013).

24. T. R. Gordon, *Fusarium oxysporum* and the *Fusarium* wilt syndrome. *Annu. Rev. Phytopathol.* **55**, 23–39 (2017).
25. R. Dean, J. A. Van Kan, Z. A. Pretorius, K. E. Hammond-Kosack, A. Di Pietro, P. D. Spanu, J. J. Rudd, M. Dickman, R. Kahmann, J. Ellis, G. D. Foster, The top 10 fungal pathogens in molecular plant pathology. *Mol. Plant Pathol.* **13**, 414–430 (2012).
26. Y. Wang, R. N. Pruitt, T. Nürnberger, Y. C. Wang, Evasion of plant immunity by microbial pathogens. *Nat. Rev. Microbiol.* **20**, 449–464 (2022).
27. J. D. G. Jones, B. J. Staskawicz, J. L. Dangl, The plant immune system: From discovery to deployment. *Cell* **187**, 2095–2116 (2024).
28. P. N. Dodds, J. P. Rathjen, Plant immunity: Towards an integrated view of plant-pathogen interactions. *Nat. Rev. Genet.* **11**, 539–548 (2010).
29. L. J. Ma, H. C. van der Does, K. A. Borkovich, J. J. Coleman, M. J. Daboussi, A. Di Pietro, M. Dufresne, M. Freitag, M. Grabherr, B. Henrissat, P. M. Houterman, S. Kang, W. B. Shim, C. Woloshuk, X. Xie, J. R. Xu, J. Antoniw, S. E. Baker, B. H. Bluhm, A. Breakspear, D. W. Brown, R. A. Butchko, S. Chapman, R. Coulson, P. M. Coutinho, E. G. Danchin, A. Diener, L. R. Gale, D. M. Gardiner, S. Goff, K. E. Hammond-Kosack, K. Hilburn, A. Hua-Van, W. Jonkers, K. Kazan, C. D. Kodira, M. Koehrsen, L. Kumar, Y. H. Lee, L. Li, J. M. Manners, D. Miranda-Saavedra, M. Mukherjee, G. Park, J. Park, S. Y. Park, R. H. Proctor, A. Regev, M. C. Ruiz-Roldan, D. Sain, S. Sakthikumar, S. Sykes, D. C. Schwartz, B. G. Turgeon, I. Wapinski, O. Yoder, S. Young, Q. Zeng, S. Zhou, J. Galagan, C. A. Cuomo, H. C. Kistler, M. Rep, Comparative genomics reveals mobile pathogenicity chromosomes in *Fusarium*. *Nature* **464**, 367–373 (2010).
30. A. M. Al-Hatmi, J. F. Meis, G. S. de Hoog, *Fusarium*: Molecular diversity and intrinsic drug resistance. *PLOS Pathog.* **12**, e1005464 (2016).
31. C. Costantini, G. Renga, F. Sellitto, M. Borghi, C. Stincardini, M. Pariano, T. Zelante, F. Chiarotti, A. Bartoli, P. Mosci, L. Romani, S. Brancorsini, M. M. Bellet, Microbes in the era of circadian medicine. *Front. Cell. Infect. Microbiol.* **10**, 30 (2020).
32. G. Steed, D. C. Ramirez, M. A. Hannah, A. A. R. Webb, Chronoculture, harnessing the circadian clock to improve crop yield and sustainability. *Science* **372**, eabc9141 (2021).
33. P. Tognini, C. A. Thaiss, E. Elinav, P. Sassone-Corsi, Circadian coordination of antimicrobial responses. *Cell Host Microbe* **22**, 185–192 (2017).
34. H. Lu, C. R. McClung, C. Zhang, Tick tock: Circadian regulation of plant innate immunity. *Annu. Rev. Phytopathol.* **55**, 287–311 (2017).
35. E. van Roosmalen, C. de Bekker, Mechanisms underlying *Ophiocordyceps* infection and behavioral manipulation of ants: Unique or ubiquitous? *Annu. Rev. Microbiol.* **78**, 575–593 (2024).
36. C. de Bekker, B. Das, Hijacking time: How *Ophiocordyceps* fungi could be using ant host clocks to manipulate behavior. *Parasite Immunol.* **44**, e12909 (2022).
37. L. Salichos, A. Rokas, The diversity and evolution of circadian clock proteins in fungi. *Mycologia* **102**, 269–278 (2010).
38. L. F. Larrondo, J. J. Loros, J. C. Dunlap, High-resolution spatiotemporal analysis of gene expression in real time: In vivo analysis of circadian rhythms in *Neurospora crassa* using a FREQUENCY-luciferase translational reporter. *Fungal Genet. Biol.* **49**, 681–683 (2012).
39. Y. Liu, M. Merrow, J. J. Loros, J. C. Dunlap, How temperature changes reset a circadian oscillator. *Science* **281**, 825–829 (1998).
40. H. Peng, Y. L. Zhang, S. H. Ying, M. G. Feng, The essential and the nonessential roles of four clock elements in the circadian rhythm of *Metarhiziumrobertsii*. *J. Fungi.* **8**, 558 (2022).
41. S. M. Tong, D. Y. Wang, Q. Cai, S. H. Ying, M. G. Feng, Opposite nuclear dynamics of two FRH-dominated frequency proteins orchestrate non-rhythmic conidiation in *Beauveria bassiana*. *Cells* **9**, 626 (2020).
42. K. Lee, J. J. Loros, J. C. Dunlap, Interconnected feedback loops in the *Neurospora* circadian system. *Science* **289**, 107–110 (2000).
43. B. D. Aronson, K. A. Johnson, J. J. Loros, J. C. Dunlap, Negative feedback defining a circadian clock: Autoregulation of the clock gene frequency. *Science* **263**, 1578–1584 (1994).
44. X. L. Liu, Z. Duan, M. Yu, X. Liu, Epigenetic control of circadian clocks by environmental signals. *Trends Cell Biol.* **34**, 992–1006 (2024).
45. J. M. Hurley, M. S. Jankowski, H. De Los Santos, A. M. Crowell, S. B. Fordyce, J. D. Zucker, N. Kumar, S. O. Purvine, E. W. Robinson, A. Shukla, E. Zink, W. R. Cannon, S. E. Baker, J. J. Loros, J. C. Dunlap, Circadian proteomic analysis uncovers mechanisms of post-transcriptional regulation in metabolic pathways. *Cell Syst* **7**, 613–626.e5 (2018).
46. Q. Zuriegat, Y. R. Zheng, H. Liu, Z. H. Wang, Y. Z. Yun, Current progress on pathogenicity-related transcription factors in *Fusarium oxysporum*. *Mol. Plant Pathol.* **22**, 882–895 (2021).
47. J. M. Hurley, A. Dasgupta, J. M. Emerson, X. Zhou, C. S. Ringelberg, N. Knabe, A. M. Lipzen, E. A. Lindquist, C. G. Daum, K. W. Barry, I. V. Grigoriev, K. M. Smith, J. E. Galagan, D. Bell-Pedersen, M. Freitag, C. Cheng, J. J. Loros, J. C. Dunlap, Analysis of clock-regulated genes in *Neurospora* reveals widespread posttranscriptional control of metabolic potential. *Proc. Natl. Acad. Sci. U.S.A.* **111**, 16995–17002 (2014).
48. A. Goity, A. Dovzhenok, S. Lim, C. Hong, J. Loros, J. C. Dunlap, L. F. Larrondo, Transcriptional rewiring of an evolutionarily conserved circadian clock. *EMBO J.* **43**, 2015–2034 (2024).
49. C. Sancar, G. Sancar, N. Ha, F. Cesbron, M. Brunner, Dawn- and dusk-phased circadian transcription rhythms coordinate anabolic and catabolic functions in *Neurospora*. *BMC Bio* **13**, 17 (2015).
50. K. M. Smith, G. Sancar, R. Dekhang, C. M. Sullivan, S. Li, A. G. Tag, C. Sancar, E. L. Bredeweg, H. D. Priest, R. F. McCormick, T. L. Thomas, J. C. Carrington, J. E. Stajich, D. Bell-Pedersen, M. Brunner, M. Freitag, Transcription factors in light and circadian clock signaling networks revealed by genomewide mapping of direct targets for *Neurospora* White Collar complex. *Eukaryot. Cell* **9**, 1549–1556 (2010).
51. A. Cimmino, M. Masi, M. Evidente, S. Superchi, A. Evidente, Fungal phytotoxins with potential herbicidal activity: Chemical and biological characterization. *Nat. Prod. Rep.* **32**, 1629–1653 (2015).
52. J. Macheleidt, D. J. Mattern, J. Fischer, T. Netzker, J. Weber, V. Schroeckh, V. Valiante, A. A. Brakhage, Regulation and role of fungal secondary metabolites. *Annu. Rev. Genet.* **50**, 371–392 (2016).
53. Y. Yun, X. Zhou, S. Yang, Y. Wen, H. You, Y. Zheng, J. Norvienyeku, W. B. Shim, Z. Wang, *Fusarium oxysporum* f. sp. *lycopersici* C_2H_2 transcription factor FolCzf1 is required for conidiation, fusaric acid production, and early host infection. *Curr. Genet.* **65**, 773–783 (2019).
54. A. Gutierrez-Sanchez, J. Plasencia, J. L. Monribot-Villanueva, B. Rodriguez-Haas, E. Ruiz-May, J. A. Guerrero-Analco, D. Sanchez-Rangel, Virulence factors of the genus *Fusarium* with targets in plants. *Microbiol. Res.* **277**, 127506 (2023).
55. S. M. Tong, B. J. Gao, H. Peng, M. G. Feng, Essential roles of two FRQ proteins (Frq1 and Frq2) in *Beauveria bassiana*'s virulence, infection cycle, and calcofluor-specific signaling. *Appl. Environ. Microbiol.* **87**, e02545-20 (2021).
56. F. Halberg, E. A. Johnson, B. W. Brown, J. J. Bittner, Susceptibility rhythm to *E. coli* endotoxin and bioassay. *Proc. Soc. Exp. Biol. Med.* **103**, 142–144 (1960).
57. P. G. Shackelford, R. D. Feigin, Periodicity of susceptibility to pneumococcal infection: Influence of light and adrenocortical secretions. *Science* **182**, 285–287 (1973).
58. K. Man, A. Loudon, A. Chawla, Immunity around the clock. *Science* **354**, 999–1003 (2016).
59. H. Borrmann, F. Rijo-Ferreira, Crosstalk between circadian clocks and pathogen niche. *PLOS Pathog.* **20**, e1012157 (2024).
60. M. M. Bellet, E. Deriu, J. Z. Liu, B. Grimaldi, C. Blaschitz, M. Zeller, R. A. Edwards, S. Sahar, S. Dandekar, P. Baldi, M. D. George, M. Raffatellu, P. Sassone-Corsi, Circadian clock regulates the host response to *Salmonella*. *Proc. Natl. Acad. Sci. U.S.A.* **110**, 9897–9902 (2013).
61. W. Wang, J. Y. Barnaby, Y. Tada, H. Li, M. Tor, D. Caldelari, D. U. Lee, X. D. Fu, X. Dong, Timing of plant immune responses by a central circadian regulator. *Nature* **470**, 110–114 (2011).
62. C. R. McClung, Plant biology: Defence at dawn. *Nature* **470**, 44–45 (2011).
63. A. M. Curtis, M. M. Bellet, P. Sassone-Corsi, L. A. O'Neill, Circadian clock proteins and immunity. *Immunity* **40**, 178–186 (2014).
64. P. Zhu, A. Idnurm, The contribution of the White Collar complex to *Cryptococcus neoformans* virulence is independent of its light-sensing capabilities. *Fungal Genet. Biol.* **121**, 56–64 (2018).
65. A. M. M. Tiley, C. Lawless, P. Pilo, S. J. Karki, J. Lu, Z. Long, H. Gibriel, A. M. Bailey, A. Feechan, The *Zymoseptoria tritici white collar-1* gene, *ZtWco-1*, is required for development and virulence on wheat. *Fungal Genet. Biol.* **161**, 103715 (2022).
66. M. C. Ruiz-Roldan, V. Garre, J. Guarro, M. Marine, M. I. Roncero, Role of the white collar 1 photoreceptor in carotenogenesis, UV resistance, hydrophobicity, and virulence of *Fusarium oxysporum*. *Eukaryot. Cell* **7**, 1227–1230 (2008).
67. Y. Tang, P. Zhu, Z. Lu, Y. Qu, L. Huang, N. Zheng, Y. Wang, H. Nie, Y. Jiang, L. Xu, The photoreceptor components FaWC1 and FaWC2 of *Fusarium asiaticum* cooperatively regulate light responses but play independent roles in virulence expression. *Microorganisms* **8**, 365 (2020).
68. D. J. Eide, Transcription factors and transporters in zinc homeostasis: Lessons learned from fungi. *Crit. Rev. Biochem. Mol. Biol.* **55**, 88–110 (2020).
69. M. S. Lopez-Berges, ZafA-mediated regulation of zinc homeostasis is required for virulence in the plant pathogen *Fusarium oxysporum*. *Mol. Plant Pathol.* **21**, 244–249 (2020).
70. M. A. Moreno, O. Ibrahim-Granet, R. Vicentefranqueira, J. Amich, P. Ave, F. Leal, J. P. Latge, J. A. Calera, The regulation of zinc homeostasis by the ZafA transcriptional activator is essential for *Aspergillus fumigatus* virulence. *Mol. Microbiol.* **64**, 1182–1197 (2007).
71. A. Djamei, K. Schipper, F. Rabe, A. Ghosh, V. Vincon, J. Kahnt, S. Osorio, T. Tohge, A. R. Fernie, I. Feussner, K. Feussner, P. Meinicke, Y. D. Stierhof, H. Schwarz, B. Macek, M. Mann, R. Kahmann, Metabolic priming by a secreted fungal effector. *Nature* **478**, 395–398 (2011).
72. L. Xie, Y. Bi, C. He, J. Situ, M. Wang, G. Kong, P. Xi, Z. Jiang, M. Li, Unveiling microRNA-like small RNAs implicated in the initial infection of *Fusarium oxysporum* f. sp. *cubense* through small RNA sequencing. *Mycology* 1–16 (2024).
73. N. Li, S. Kang, Do volatile compounds produced by *Fusarium oxysporum* and *Verticillium dahliae* affect stress tolerance in plants? *Mycology* **9**, 166–175 (2018).
74. C. Hua, J. H. Zhao, H. S. Guo, Trans-kingdom RNA silencing in plant-fungal pathogen interactions. *Mol. Plant* **11**, 235–244 (2018).

75. J. Collemare, R. O'Connell, M. H. Lebrun, Nonproteinaceous effectors: The *terra incognita* of plant–fungal interactions. *New Phytol.* **223**, 590–596 (2019).
76. N. P. Keller, G. Turner, J. W. Bennett, Fungal secondary metabolism — From biochemistry to genomics. *Nat. Rev. Microbiol.* **3**, 937–947 (2005).
77. M. Gao, C. Xiong, C. Gao, C. K. M. Tsui, M. M. Wang, X. Zhou, A. M. Zhang, L. Cai, Disease-induced changes in plant microbiome assembly and functional adaptation. *Microbiome* **9**, 187 (2021).
78. J. E. Leach, L. R. Triplett, C. T. Argueso, P. Trivedi, Communication in the Phytobiome. *Cell* **169**, 587–596 (2017).
79. X. Jin, H. Jia, L. Ran, F. Wu, J. Liu, K. Schlaeppi, F. Dini-Andreote, Z. Wei, X. Zhou, Fusaric acid mediates the assembly of disease-suppressive rhizosphere microbiota via induced shifts in plant root exudates. *Nat. Commun.* **15**, 5125 (2024).
80. H. G. Wen, J. H. Zhao, B. S. Zhang, F. Gao, X. M. Wu, Y. S. Yan, J. Zhang, H. S. Guo, Microbe-induced gene silencing boosts crop protection against soil-borne fungal pathogens. *Nat. Plants.* **9**, 1409–1418 (2023).
81. X. Zhou, J. Wang, F. Liu, J. Liang, P. Zhao, C. K. M. Tsui, L. Cai, Cross-kingdom synthetic microbiota supports tomato suppression of Fusarium wilt disease. *Nat. Commun.* **13**, 7890 (2022).
82. V. D. Gooch, A. Mehra, L. F. Larrondo, J. Fox, M. Touroutoutoudis, J. J. Loros, J. C. Dunlap, Fully codon-optimized *luciferase* uncovers novel temperature characteristics of the *Neurospora* clock. *Eukaryot. Cell* **7**, 28–37 (2008).
83. X. L. Liu, Y. Yang, Y. Hu, J. Wu, C. Han, Q. Lu, X. Gan, S. Qi, J. Guo, Q. He, Y. Liu, X. Liu, The nutrient-sensing GCN2 signaling pathway is essential for circadian clock function by regulating histone acetylation under amino acid starvation. *eLife* **12**, e85241 (2023).
84. X. Liu, Y. K. Dang, T. Matsu-ura, Y. B. He, Q. He, C. I. Hong, Y. Liu, DNA replication is required for circadian clock function by regulating rhythmic nucleosome composition. *Mol. Cell* **67**, 203–213.e4 (2017).
85. N. Zhang, L. Song, Y. Xu, X. Pei, B. F. Luisi, W. Liang, The decrotonylase FoSir5 facilitates mitochondrial metabolic state switching in conidial germination of *Fusarium oxysporum*. *eLife* **10**, e75583 (2021).
86. M. J. Kwak, H. G. Kong, K. Choi, S. K. Kwon, J. Y. Song, J. Lee, P. A. Lee, S. Y. Choi, M. Seo, H. J. Lee, E. J. Jung, H. Park, N. Roy, H. Kim, M. M. Lee, E. M. Rubin, S. W. Lee, J. F. Kim, Rhizosphere microbiome structure alters to enable wilt resistance in tomato. *Nat. Biotechnol.* **36**, 1100–1109 (2018).

Acknowledgments: We thank L. Wang, C. Jin, J. Guo, and members of our laboratory for the assistance. **Funding:** This work was supported by grants from the Beijing Natural Science Foundation (JQ24034 to X.L.), the Strategic Priority Research Program of the Chinese Academy of Sciences (XDB0810000 to X.L.), and the National Natural Science Foundation of China (32370084 and 32170092 to X.L.; 32470107 to X.S.; 32200056 to X.-L.L.; 32170560 to Q.H.; and 32470609 and 32171262 to Y.D.). The funders had no role in the study design, data analysis, or preparation of the manuscript. **Author contributions:** Conceptualization: X.L., Q.L., M.Y., and X.X. Methodology: Q.L., M.Y., R.Z., and Z.L. Investigation: Q.L., M.Y., X.S., R.Z., Y.Z., Z.L., and Y.D. Visualization: Q.L., M.Y., Y.L., and X.L. Software: Q.L. Formal analysis: X.L., Q.L., M.Y., X.S., X.Z., X.-L.L., and Y.D. Data curation: Q.L., M.Y., and X.-L.L. Validation: Q.L., M.Y., Z.L., and Y.D. Funding acquisition: X.L., X.S., X.-L.L., Q.H., and Y.D. Project administration: X.L., M.Y., and Y.D. Resources: X.L., Q.H., L.C., X.Z., H.L., S.L., Y.D., and Y.L. Supervision: X.L. Writing—original draft: X.L., Y.L., Q.L., and M.Y. Writing—review and editing: X.L., Y.L., Q.L., M.Y., and X.X. **Competing interests:** The authors declare that they have no competing interests. **Data and materials availability:** All data needed to evaluate the conclusions in the paper are present in the paper and/or the Supplementary Materials. Our generated RNA-seq raw data have been deposited in the NCBI under BioProjects PRJNA1167353 and PRJNA1182093.

Submitted 23 November 2024
Accepted 25 February 2025
Published 28 March 2025
10.1126/sciadv.ads1341